Proceedings of CONF-APMM 2026 Symposium: Quantum Communication and Model Simulation
DOI: 10.54254/2753-8818/2026.GL35281

Analysis of Relationship Between the Rate of Temperature Change of Heat-Conductive Metal and the Velocity of Fluid Through Convective Heat Transfer Process

Yinji Zhao

Faculty of Engineering, University of Bristol, Bristol, UK
zhaoyinji615@163.com

Abstract. Heat transfer-related theories are crucial in practical engineering manufacturing processes, particularly in designing heating system and mechanical structures. This paper explores how convective heat transfer and fluid dynamics could be specifically related by demonstrating the proportional relation between the velocity of moving fluid and the rate of change in temperature of heat-conductive metal as the result of the heat effect by the fluid. A theoretical model for velocity-dependent expression is developed based on Nusselt, Reynolds and Prandtl's number, associated with Newton's Law of Cooling. An experiment is conducted using a hair dryer with different air speed settings, which are applied to a hollow stainless-steel metal ball, with 3 trials of data completed and recorded by a K-type thermocouple. The result demonstrates that higher fluid velocity leads to faster change in rate of temperature. This paper provides fundamental knowledge for engineering designs and applications like heat exchange systems and material selections for metal components.

Keywords: Heat transfer, velocity, temperature, fluid

1. Introduction

Nowadays, applications of fluids associated with heat transfer explorations potentially enhance efficiency in temperature in change. For example, nanofluid analysis focuses on increasing the rate of temperature change using a mixture of regular fluid and microscopic metal particles, eventually increasing the efficiency of removing heat [1]. However, the dynamics between contacting interfaces of solid and liquid might be a challenging, unexplored area in current studies. In addition, selections of materials with consideration of cooling rate and fluid properties are crucial insights in thermal-related engineering designs. Based on the up-to-date information, this paper focuses on investigating the impact of the velocity of regular fluid, air, and the rate of temperature change of solid metal surface. This is a basic demonstration process, whereas it is a fundamental analysis before many extensive studies about the complexity of intelligent designs.

© 2026 The Authors. This is an open access article distributed under the terms of the Creative Commons Attribution License 4.0 (https://creativecommons.org/licenses/by/4.0/).

DOI: 10.54254/2753-8818/2026.GL35281

2. Concepts and theories

2.1. Teoretical inferences

The fundamental concept of Nusselt number (Nu) is vital to be introduced [2]. It characteristically represents the relationship between convective heat transfer ($\alpha \Delta T$) and heat transferred by conduction ($\alpha \frac{\Delta T}{L}$). It tells how effective the convective heat transfer generated by fluid motion is compared to the heat transfer by conduction only. The formula is shown in equation (1):

$$Nu = \frac{\alpha L}{\lambda} = \frac{\alpha \Delta T}{\lambda \frac{\Delta T}{L}} \tag{1}$$

Where Nu is the Nusselt number, α represents the convective heat transfer coefficient, L is the characteristic length, and λ represents the thermal conductivity of the corresponding fluid involved.

However, the velocity of the moving fluid is related to the Reynolds number (Re), which the Nusselt number is depended on [3]. The formula of the Reynolds number is given in equation (2). It is the ratio between inertia force and viscous force. If the estimated numerical value of Reynolds number is less than 2000, it indicates that the flow is laminar and viscous force-dominated; otherwise, it indicates that the flow is turbulent and viscous force-dominated.

$$Re = \frac{\rho v L}{\mu} \tag{2}$$

ρ is the density of fluid, v is the velocity of fluid, L is the characteristic length of fluid in a particular system and μ is the viscous viscosity of fluid.

Additionally, Prandtl number is a crucial consideration related to diffusivity of heat [4]. The formula is displayed in equation (3):

$$Pr = \frac{\mu c_p}{\lambda} \tag{3}$$

μ is the dynamic viscosity, c_p is the specific heat capacity of fluid at constant pressure, λ is the thermal conductivity of the fluid.

The general formula containing all three numbers represented in equation (4) shows a dimensionless correlation for effectiveness of heat transfer in convective flow of a specific fluid over a sphere [5].

$$Nu = 2 + (0.4Re^{\frac{1}{2}} + 0.06Re^{\frac{2}{3}})Pr^{0.4} \tag{4}$$

Furthermore, to specifically investigate the relationship between fluid velocity and rate of change in fluid temperature, the Newton's law of cooling is applied, indicating that the rate of heat loss is directly proportional to the temperature difference between an object and surrounding environments [6]. Equation (5) shows an extension of Newton's law of cooling by applying energy balance.

$$mc_p \frac{dT}{dt} = \alpha A\left(T_{air} - T_s\right) \tag{5}$$

Where m is the mass of the metal ball measured in kg.

DOI: 10.54254/2753-8818/2026.GL35281

By rearranging and substituting corresponding terms from equations (1), (2), (3), (4) and (5), the equation is simplified and shown in equation (6), which clearly showes the direct proportional relation between the effectiveness of convective heat transfer and the velocity-dependent term. K, a and b are simplified terms representing various combined terms.

$$\frac{dT}{dt} = K(T_{air} - T_s)(2 + av^{\frac{1}{2}} + bv^{\frac{2}{3}}) \tag{6}$$

$$K = \frac{\lambda A}{Lmc_p} \tag{7}$$

$$a = 0.4\left(\frac{\rho L}{\mu}\right)^{\frac{1}{2}} Pr^{0.4} \tag{8}$$

$$b = 0.06\left(\frac{\rho L}{\mu}\right)^{\frac{2}{3}} Pr^{0.4} \tag{9}$$

$(T_{air} - T_s)$ represents the temperature difference between instantaneous temperature of air and surrounding environment.

2.2. Assumptions

As a result, by comparing equations (5) and (6), the theoretical hypothesis was developed that the velocity-dependent term $\left(2 + av^{\frac{1}{2}} + bv^{\frac{2}{3}}\right)$ is directly proportional to the rate of temperature change. Therefore, the assumptions of the experiment were decided as shown below.

A hollow metal ball made of 201 stainless steel was used as the object influenced by airflow. The density of 201 stainless steel, which is the material used for the metal ball, was assumed to be 7900 kg/m^3 [7]. The mass of the hollow metal ball was estimated by assuming the wall thickness as 0.0005 m and diameter of 0.063 m, resulting in the estimated value of mass of 0.04847 kg . Frictions in between the airflow were negligible. The density of air was assumed to be 1.204 kg/m^3 [8]. All physical properties were kept constant. The viscosity of fluid outside the boundary layer is negligible for all trials of predetermined velocity. The airflow was considered as a flow exerted over the external spherical shape of the metal ball. Efficiency of energy conservation between fluid and object was assumed to be 100% (no heat loss to the surroundings).

Additionally, the final steady-state temperature of the ball surface was assumed to be equal to the temperature of airflow for each velocity level since the air temperature was considered constant throughout the experiment. The reason was that the rate of heat transfer between airflow and metal ball surface approached zero when the temperature difference gradually reduced to zero, whereas the measurement of airflow temperature was not necessarily included in the experiment; therefore the steady-state temperature was allowed to be used as an effective ambient temperature.

Due to the thin shell and high heat conductivity over the internal surface of the metal ball, the lumped capacitance model is applicable, which means the temperature gradient of the interior of the ball is negligible [9]. It implies that the Biot number is expected to be small (Bi<1) to satisfy the experimental condition [10]. Thus, the temperature of the metal ball was assumed to be uniform.

DOI: 10.54254/2753-8818/2026.GL35281

3. Experimental processes

3.1. Setups

Figure 1 shows the apparatuses used for the experiment and the processes of data collections was shown below.

First, the air outlet of the hair dryer is positioned at the same level as the metal ball on the ground. The position is unchanged throughout the experiment. The specific distance between hair dryer and the metal ball was not explicitly specified since the only independent variable in this case was the fluid velocity.

Subsequently, a metal ball was stabilised at the stationary point on the ground, stuck and connected to the thermocouple with thin tapes. The position of the metal ball was unchanged throughout the experiment. TA612C K-type thermometer was used to detect the instantaneous changes of temperature, where the initial temperature displayed after activation was the room temperature [11]. It is stuck and connected with the surface of the metal ball. Two values of temperature are displayed and the average of the results was used for analysis. Additionally, the stop watch was used in order to obtain the time period when the change of temperature happens. An additional device was used to record videos of the processes of the experiment.



Figure 1. Experimental preparations and apparatus

3.2. Experiment procedures

First, ensure the hair dryer and metal ball are positioned appropriately and keep the position until the end of all trials of experiment. Second, plug the input jacks onto the thermometer and connect the thermocouple probes. Activate the thermometer by pressing and holding the button for turning on. After that, start recording the video of all setups including the stop watch. Then, activate the stop watch after starting recording the video. Next, adjust the heat level of the hair dryer to maximum, keep it unchanged, then turn on the hair dryer and set the level of air power to the first level. Observe the change of temperature on the thermometer and stop the recording until no further noticeable data changes on the thermometer. Subsequently, turn off the thermometer, stay still for 5 minutes to ensure the temperature of the metal ball is decreased to room temperature. After all of the

DOI: 10.54254/2753-8818/2026.GL35281

steps, repeat steps 4 to 8, setting the level of air power to the second level in step 6. Finally, repeat steps 4 to 8, setting the level of air power to the third level in step 6.

3.3. Experimental results

The raw data collected from the experiment on the change of temperature of the surface of the metal ball with time was shown in Figure 2. Three levels of velocities of airflow were used in order to demonstrate the relation between theoretical hypothesis and practical trends.

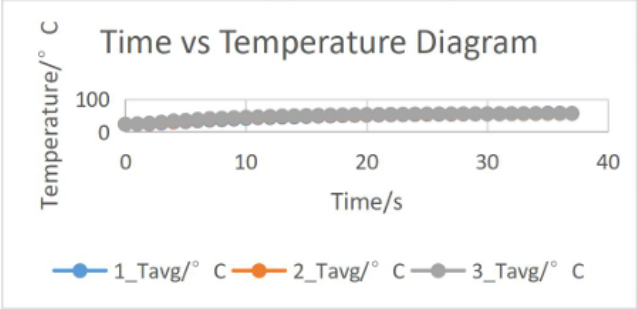


Figure 2. Time against temperature diagram

Figure 2 illustrates the time taken for the temperature of the metal ball to reach the maximum temperature against temperature values raised from room temperature to the final value under three respective velocity levels. All three curves show that temperature increases relatively fast at initial stage and the rate of increase in temperature reduces gradually when approaching maximum steady-state temperature.

4. Discussion

4.1. Data analysis

Figure 2 shows a non-linear physical trend of the results. By observation, the temperature rose at a greater rate at first, which means $\frac{dT}{dt}$ was greater, therefore resulting in a greater heat transfer rate. Then the rate of increase in temperature reduced gradually as temperature approached the steady-state temperature at the sphere. Therefore, there was an insignificant increase in temperature at the final stage, resulting in an extremely slow rate of temperature change.

By comparing the general trend of curves, the temperature "3_Tavg," influenced by the maximum velocity level, reached steady-state temperature the fastest, followed by "2_Tavg" with the second velocity level, and "1_Tavg" reached the steady-state temperature the slowest. This phenomenon reflected that the velocities factor $\left(av^{\frac{1}{2}}+bv^{\frac{2}{3}}\right)$ in equation (6) was directly related to Nusselt number, which led to an increase in convective heat transfer and therefore increased $\frac{dT}{dt}$. However, the non-linear result could not directly illustrate the relation between velocity of airflow and rate of temperature change. The Biot number calculation is presented in equation (10) to verify the validity of assumption in section 2.2. The thermal conductivity for the particular material of ball used in the experiment was 16.2 W/m K [12].

$$Bi=\frac{(0.04847)\times500\times(24.8-23.7)\times(\frac{0.063}{6})}{(4\pi\times0.0315^2)\times(56.4-23.5)\times16.2}\approx0.042 \tag{10}$$

DOI: 10.54254/2753-8818/2026.GL35281

This reflected that the lumped capacitance model was reasonable for the feasibility of experiment. However, to be emphasized, this calculation assumed a solid metal sphere. Instead, a hollow sphere was used in the experiment with thickness of 0.5 mm with a result of value of Biot number of approximately 0.003, which further confirmed the validity of the assumption in section 2.2.

4.2. Further evaluations

The further extensions of the data collected were shown in Figures 3 and 4 using Python code. An average of initial and final temperature of ball surface of all trials was calculated as 23.51666667℃ and 56.36666667℃ respectively.

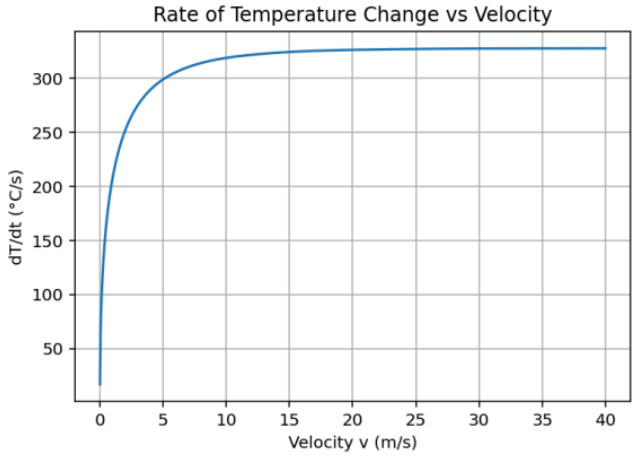


Figure 3. Graph of dT/dt and velocity of from python code

The $\frac{dT}{dt}$ against velocity graph in Figure 3 intuitively showed an exponential trend and demonstrated Newton's law of cooling, which was clearly in line with the experimental data trend.

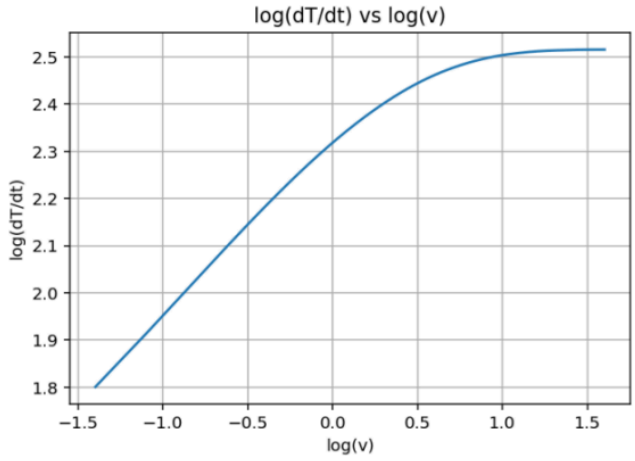


Figure 4. log(dTdt) vs log(v) graph from python code

Since $\left(2+av^{\frac{1}{2}}+bv^{\frac{2}{3}}\right)$ was a mixture of constant and power term, the relation was not linear thus no single gradient could be obtained. Therefore, in Figure 4, a log-log graph was plotted which

DOI: 10.54254/2753-8818/2026.GL35281

further clarified the gradients indicated with change of velocity. The graph also showed a general increasing trend of gradients of $\log\left(\frac{dT}{dt}\right)$.

A mathematical demonstration of slope was shown below in equation (11):

$$\frac{d\log\left(\frac{dT}{dt}\right)}{d\log(v)} = \frac{\frac{1}{2}av^{\frac{1}{2}}+\frac{2}{3}bv^{\frac{2}{3}}}{2+av^{\frac{1}{2}}+bv^{\frac{2}{3}}} \tag{11}$$

Equation (11) was derived from the theoretical model instead of the limited data from experiment. From equation (11), the simultaneous contribution of $v^{\frac{1}{2}}$ and $v^{\frac{2}{3}}$ terms indicated the coexistence of laminar and turbulent flow and was reflected in a transition regime. This made the curve approximately linear but not strictly constant when the velocity was moderately high. The influence of turbulent term $v^{\frac{2}{3}}$ eventually dominated since the $v^{\frac{2}{3}}$ grew faster due to greater power $\frac{2}{3}$. When velocity was extremely high, there was only slight increase in gradient, which consequently approached a constant of $\frac{2}{3}$ due to the gradual, fully-developed forced convection heat transfer [13].

The existence of multiple gradients at different velocity stages was in association with Reynolds number and reflected different regimes. From equation (2), Reynolds number is directly proportional to airflow velocity. As velocity increased, boundary layer of airflow became thinner as laminar flow turned into turbulent due to an increase in Reynolds number.

Also, in equation (6), $v^{\frac{1}{2}}$ term reflected a laminar-dominated regime of convection of flow. Physically, this term dominated during heat transfer when airflow was slow and smooth. $v^{\frac{2}{3}}$ indicated a turbulent-dominated regime of convection due to the increase in velocity. This term dominated the heat transfer process during transition or turbulent state. When $\left(av^{\frac{1}{2}}+bv^{\frac{2}{3}}\right)$ is small, natural convection dominates the transfer process. The combined term elucidates the transition of flow from laminar to turbulents, which implies the gradual increasing trend of heat transfer coefficient and hence the heat transfer rate, leading to a higher rate of temperature change.

4.3. Improvements

The experiment demonstrated theoretical trends and provided persuasive explanations of the correlation between velocity of airflow and rate of change in temperature over the convective heat transfer process. However, some details could be improved to enhance the quality of experiment.

First, it is acknowledged that all three curves from Figure 3 showed the same general trends and reliable ending points. However, only three limited experimental results would not satisfy the persuasive demonstration of quantitative knowledge. This potentially led to insufficient data, existence of biased values and negative influences on precision of representing trends. Therefore, the data obtained from the experiment is only a qualitative demonstration of the model inferred, and should be considered as supportive evidence. For more valid and definitive confirmation of reliability of the velocity-dependent expression, a greater number of velocity levels could be used in order to obtain more opportunities for comparing temperature change over time. Instead of using a hair dryer, a more precise, accurate device with more ranges of velocity levels and temperature settings could be applied. For example, a TecQuipment AF1300 Subsonic Wind Tunnel could be considered since it has a continuous speed setting function rather than prefixed speed levels, which is the ideal case to investigate the trend of this experiment [14].

DOI: 10.54254/2753-8818/2026.GL35281

The final steady-state temperature of the ball surface was taken and assumed to be equal to the final air temperature since the experiment was aimed at focusing on rate of change in temperature. For acquirement of results with high accuracy, the temperature of airflow could be measured using the same type of thermocouples by avoiding contact with the surfaces of devices.

Also, all the physical properties of air and metal ball were changed slightly due to the change in temperature. This would result in inaccuracy of error considerations and precision of extrapolations of graphs. Further research about corresponding densities of metal ball and airflow and dynamic viscosity of airflow at different temperatures could be done and corresponding graphs could be plotted if needed. In addition, the friction of airflow from the outlet of hair dryer and in between the hair dryer and metal ball was assumed to be zero. However, the airflow was potentially unsteady and viscid in reality. The slight changes were neglected but could be potentially considered.

Furthermore, the specific distance between the hair dryer and the metal ball surface was not stated since the respective air speed and air temperature were assumed to be constant. This could be measured for more accurate heat transfer efficiency calculations if numerical values were needed for further investigations.

5. Conclusion

In conclusion, this paper investigates the relationship between fluid velocity and rate of change in temperature of a heat-conductive metal under convective heat transfer. The experimental result demonstrates that higher velocity leads to greater rate of change in temperature, which was consistent with the theoretical velocity-dependent expression.

However, some shortcomings including limited numbers and lack of values of velocity levels, tools utilized and impacts of assumptions could be improved by using high-precision machines and replacing deployment conditions. In addition, the results could be applied to heat exchange systems and new fluid development, such as connections between nanofluids and its corresponding uses in heat transfer.

References

[1] Das, P. K., Santra, A. K., Ganguly, R., Dash, S. K., Muthusamy, S., Sha, M., & Sadasivuni, K. K. (2024). An extensive review of preparation, stabilization, and application of single and hybrid nanofluids. Journal of Thermal Analysis and Calorimetry, 149(17), 9523-9557.

[2] Thermopedia. (2011). NUSSELT NUMBER. https: //thermopedia.com/content/993/

[3] The Engineering ToolBox. (2009). Reynolds Number - Laminar vs. Turbulent Flow. https: //www.engineeringtoolbox.com/reynolds-number-d_237.html

[4] Bergman, T. L. (2011). Fundamentals of heat and mass transfer. John Wiley & Sons.

[5] BYJU'S. (2024). What Is Newton's Law of Cooling? https: //byjus.com/physics/newtons-law-of-cooling/

[6] MatWeb. (2024). 201 Stainless Steel Material Property Data. https: //www.matweb.com/search/QuickText.aspx?SearchText=201+stainless+steel

[7] The Engineering ToolBox. (2003). Air Density, Specific Weight, and Thermal Expansion Coefficients at Varying Temperatures and Pressures. https: //www.engineeringtoolbox.com/air-density-specific-weight-d_600.html

[8] Voldman, J. (2007). Lumped-element Modeling with Equivalent Circuits. MIT OpenCourseWare. https: //ocw.mit.edu/courses/6-777j-design-and-fabrication-of-microelectromechanical-devices-spring-2007/resources/07lecture08/

[9] Omega Engineering. (2024). K-Type Thermocouple Technical Reference. https: //www.omega.com/en-us/resources/thermocouple-types

[10] Fakoor-Pakdaman, M., & Bahrami, M. (2013, July). Transient Internal Forced Convection Under Step Wall Heat Flux Condition. In Heat Transfer Summer Conference (Vol. 55478, p. V001T03A026). American Society of Mechanical Engineers.

DOI: 10.54254/2753-8818/2026.GL35281

[11] Aziz, S. A., Janna, W. S., & Jakubowski, G. S. (1995, November). Forced convection heat transfer from an isothermal melting ice sphere submerged in flowing water. In ASME International Mechanical Engineering Congress and Exposition (Vol. 17513, pp. 213-217). American Society of Mechanical Engineers.
[12] Combined Metals Company, LLC. (2024). 201 Stainless Steel Alloy Data Sheet. https: //www.combmet.com/wp-content/uploads/2024/01/201-Stainless-Steel-Alloy-Data-Sheet.pdf
[13] Lienhard IV, J. H., Lienhard, J. H. V., & JH, A. (2020). A Heat Transfer Textbook, Version 5.10.
[14] TecQuipment. (2025). Enhancing Engineering Education with the TecQuipment AF1300 Subsonic Wind Tunnel. https: //www.tecquipment.com/zh/case-studies/enhancing-engineering-education-with-the-tecquipment-af1300-subsonic-wind-tunnel-at-the-university-of-bedfordshire